The N501Y and K417N mutations in the spike protein of SARS-CoV-2 alter the interactions with both hACE2 and human derived antibody: A Free energy of perturbation study

Journal:	*Journal of Chemical Information and Modeling*
Manuscript ID	Draft
Manuscript Type:	Article
Date Submitted by the Author:	n/a
Complete List of Authors:	Fratev, Filip; The University of Texas at El Paso, School of Pharmacy

The N501Y and K417N Mutations in the Spike Protein of SARS-CoV-2 Alter the Interactions with Both hACE2 and Human Derived Antibody: A Free Energy of Perturbation Study

Filip Fratev[1, 2]

[1] Department of Pharmaceutical Sciences, School of Pharmacy, The University of Texas at El Paso, 1101 N Campbell St, El Paso, TX 79968, USA;

[2] Micar Innovation (Micar21) Ltd., Persenk 34B, 1407, Sofia, Bulgaria;

*Corresponding author e-mail: fffratev@utep.edu

Abstract

The N501Y and K417N mutations in spike protein of SARS-CoV-2 and their combination arise questions but the data about their mechanism of action at molecular level are limited. Here, we present Free energy perturbation (FEP) calculations for the interactions of the spike S1 receptor binding domain (RBD) with both the ACE2 receptor and an antibody derived from COVID-19 patients. Our results showed that the S1 RBD-ACE2 interactions were significantly increased whereas those with the STE90-C11 antibody dramatically decreased. The K417N mutation in a combination with N501Y fully abolished the antibody effect. However, Lys417Asn seems to have a compensatory mechanism of action increasing the S1 RBD-ACE2 free energy of binding. This may explain the observed in UK and South Africa more spread of the virus but also rose an important question about the possible human immune response and the success of already available vaccines. Notable, when the experimental data became available confirming our calculations it was demonstrated that protein-protein FEP can be a useful tool for providing urgent data to the scientific community.

Introduction

The discussion about the N501Y and K412N mutations in COVID-19 arouse many questions in the late 2020 but little data were available during this period [1]. During the last weeks of 2020, the N501Y mutation (B.1.1.7 lineage) has been mainly observed in UK whereas the combination of N501Y and K417N mutations (501Y.V2 lineage) mostly in a South Africa (SA). This led to new governmental restrictions and many countries closed their borders for the travelers coming from the UK. A little was known about the N501Y and K417N but their positions and well established interaction with the human ACE2 protein (hACE2), which is responsible for the virus entry into the cells, deserved a special attention. Moreover, it has been shown that N501Y significantly increases virus adaption in a mouse model [2]. In addition, an enhancement of the virus transmission in humans of about 70% were reported [1]. Thus, information about the molecular mechanism of action of N501Y and K417N were urgently need.

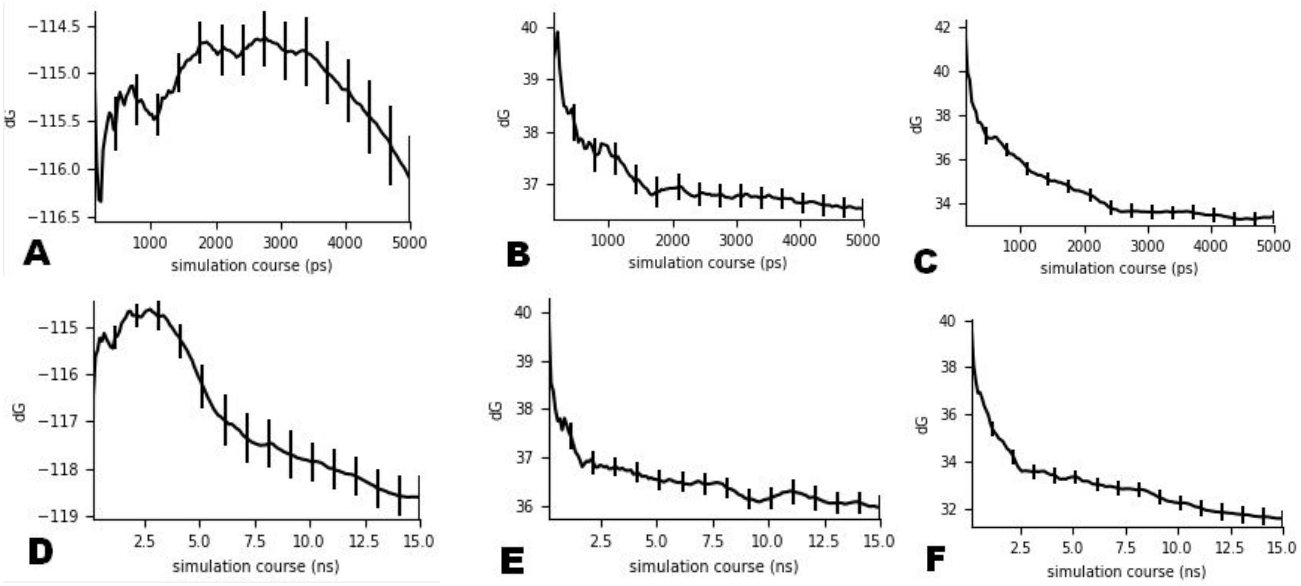

Figure 1. Observed convergence of the calculated Bennett free energies of binding for the complex legs of the mutations: ***(A)*** N501D-ACE2, ***(B)*** N501Y-STE90-C11 and ***(C)*** N501Y-ACE2, after 5 ns FEP, respectively and (***D***) N501D-ACE2 (***E***) N501Y-STE90-C11 and (***F***) N501Y-ACE2 after 15ns of the FEP simulations.

Despite the computational demands, the Free energy of binding (FEP) approach is one of the most successful and precise *in silico* techniques for accurate prediction of both the ligand selectivity [3], protein-protein interactions [4] and protein stability [5]. It outperforms significantly the traditional molecular dynamics based methodologies, such as for example MM/GBSA and empirical solutions like FoldX and etc. and often precisely predicts the free energy differences between the mutations with a RMSE of about only 1-1.5 kcal/mol [4-5]. It has been also shown that the better sampling approaches lead to much better results and most importantly for more than 90% correct predictions of the effect; i.e.

Table 1. FEP results for the selected mutations (kcal/mol). See the text for details. Energy Conv. And CCC are the Bennett and cycle closure (CC) convergence in kcal/mol^{-1}*ns^{-1}, respectively. N/A – not available

Mutation	ΔΔG Bennett (5 ns)	Energy Conv. 5 ns	CCC 5 ns	ΔΔG Bennett (15 ns)	ΔΔG CC (15 ns)	Energy Conv. 15 ns	CCC 15 ns
N501Y-STE90-C11	3.78 (0.15)	<0.1	N/A	3.48 (0.12)	N/A	<0.1	N/A
K417N-STE90-C11	5.64 (0.17)	<0.1	N/A	5.74 (0.15)	N/A	<0.1	N/A
N501Y/K417N-STE90-C11	8.61 (0.46)	<0.3	N/A	5.83 (0.43)	N/A	<0.1	N/A
K417N-ACE2	-0.39 (0.23)	<0.3	N/A	0.64 (0.21)	N/A	<0.1	N/A
N501Y-ACE2	-0.5 (0.34)	0.3	<0.8	-1.75 (0.37)	-1.42 (0.56)	<0.1	<0.5
N501D-ACE2	6.25 (0.46)	=>0.5	>0.8	3.54 (0.44)	3.22 (0.56)	<0.1	<0.5
N501T-ACE2	-1.69 (0.29)	<0.3	<0.8	-1.90 (0.17)	-2.24 (0.60)	<0.1	<0.5
N501F-ACE2	0.78 (0.27)	=>0.5	>0.8	-0.00 (0.33)	0.34 (0.60)	<0.1	<0.5

whether the effect will be positive or negative after certain ligand or protein substitutions [6].
The aim of this study was to provide urgently high quality data about the effect of the N501Y and K417N mutations in December 2020 [6]. However, during the revision process many experimental studies became available which was an excellent opportunity for a validation of the *in silico* approaches employed here and in particular FEP.

Methods

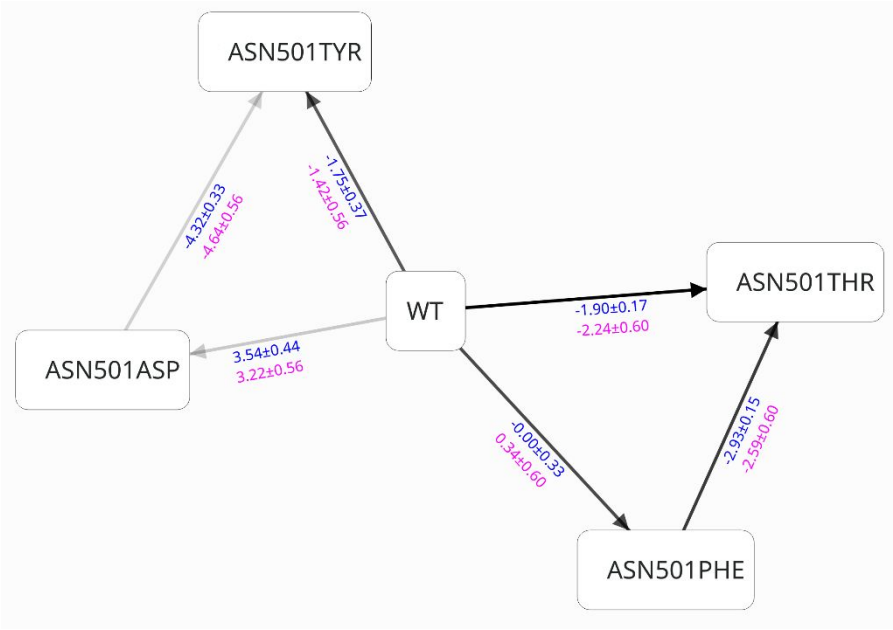

Figure 2. A schematic presentation of the perturbation networks employed for the N501 mutations. In blue and red color are shown the calculated by Bennett and cycle closure approach ΔΔG values, respectively.

To calculate the differences in the free energy of binding for each complex in this study we employed the Desmond FEP/REST approach described in details previously [5,7]. A sample scheme of the thermodynamical cycle for the calculations of the binding affinity change due to mutations in interacting protein-protein interface is shown on Figure 1 in ref [8]. The binding free energy change $\Delta\Delta G_{AB}$ or in simple ΔΔG can then be obtained from the difference between the free energy changes caused by the particular mutation in the bound state (ΔG_1, complex leg) and the unbound state i.e. in solvent (ΔG_2, solvent leg). In a typical FEP calculation for a mutation from state A to state B, several perturbation lambda (λ) windows are needed in order to obtain a smooth transition from the initial state A to the final state B. The default sampling protocol was applied with the number of λ windows either 12 or 24, in dependence of the mutation charge; i.e. same or different. An equilibration and 5 ns-long replica exchange solute tempering (REST) simulations in a muVT ensemble was further conducted. Only the mutated atoms was included in the REST "hot region" region. OPLS3e force field was used for the all simulations [9]. A set of N501 mutations for which experimental data is available was selected to validate the calculations. The experimental structure of the S1 RBD-hACE2 complex (pdb: 6M0J) was used as a starting point. After the solvation with SPC waters the complex consisted of over 102 000 atoms. For the study of S1 RBD interactions with the neutralizing antibody STE90-C11 selected from COVID-19 patients [10], which was well tolerated to the known mutations, we use the recently published X-ray structure with a PDB access number of 7B3O. For the FEP calculations with double N501Y/K417N mutations we used as a starting point the energy minimized most representative frame of the N501Y FEP/REST simulations. A regular 500ns-long MD production run was also performed in the same conditions and muVT ensemble.

Results and discussion

Table 1 presents the results from FEP calculations. As one can see the energy convergences in some cases were not so good for both the Bennett and the cycle closure (CC) approaches (see **Figures 1A**). In fact, the error of the calculated $\Delta\Delta G_{CC}$ predictions, during the first 5 ns, suffered from much larger standard deviations.

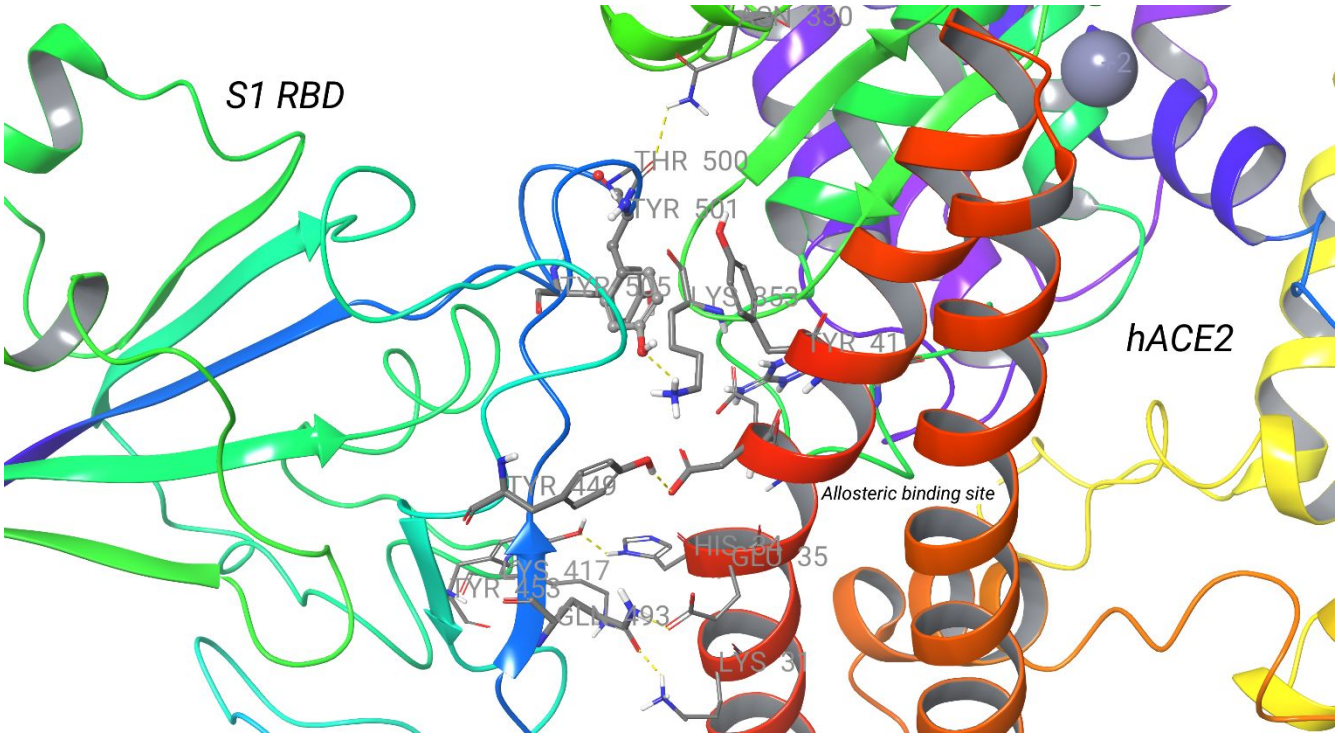

Figure 3. A close look of the identified by FEP interactions between the S1 RBD of N501Y mutant and hACE2. With yellow dot lines are shown the H-bonds.

The convergence is indeed a very important issue during the FEP calculations. Hence, we extended the FEP calculations to 15 ns-long REST sampling and obtained a good convergence (see **Table 1** and **Figure 1D**). A schematic presentation of the perturbation networks and calculated ΔΔG values for the selected set of N501 mutations are also shown (**Figure 2**).

The cycle closure calculations for protein-protein selectivity have been not studied well, thus, to avoid any confusions in the interpretations we used only the Bennett values to make our conclusions herein. Moreover, during the initial phase of our study the K417N mutation was not reported yet and it was difficult to obtain the $\Delta\Delta G_{CC}$ values for the S1 RBD-STE90-C11 complex at this stage. The better sampling protocols could make the free energies more precise and improve the CC ΔΔG values, however, it is not likely to change qualitatively the results present here [7]; i.e. whether one mutation results either in an increase or decrease in the interactions. This conclusion is also based on our experience with such type of simulations with both the ligand-protein complexes and protein mutations [7, 11].

The main results of the FEP study were:

1) We observed significant decrease of the binding between S1 RBD and STE90-C11 antibody by ΔΔG of 3.78 kcal/mol after 5ns of FEP/REST simulations. This is a significant value and the observed convergence was good (**Table 1** and **Figures 1B** and **1E**). The binding energy of the antibody can be roughly estimated based on the published value of IC_{50}=0.56nM in a plaque-based live SARS-CoV-2

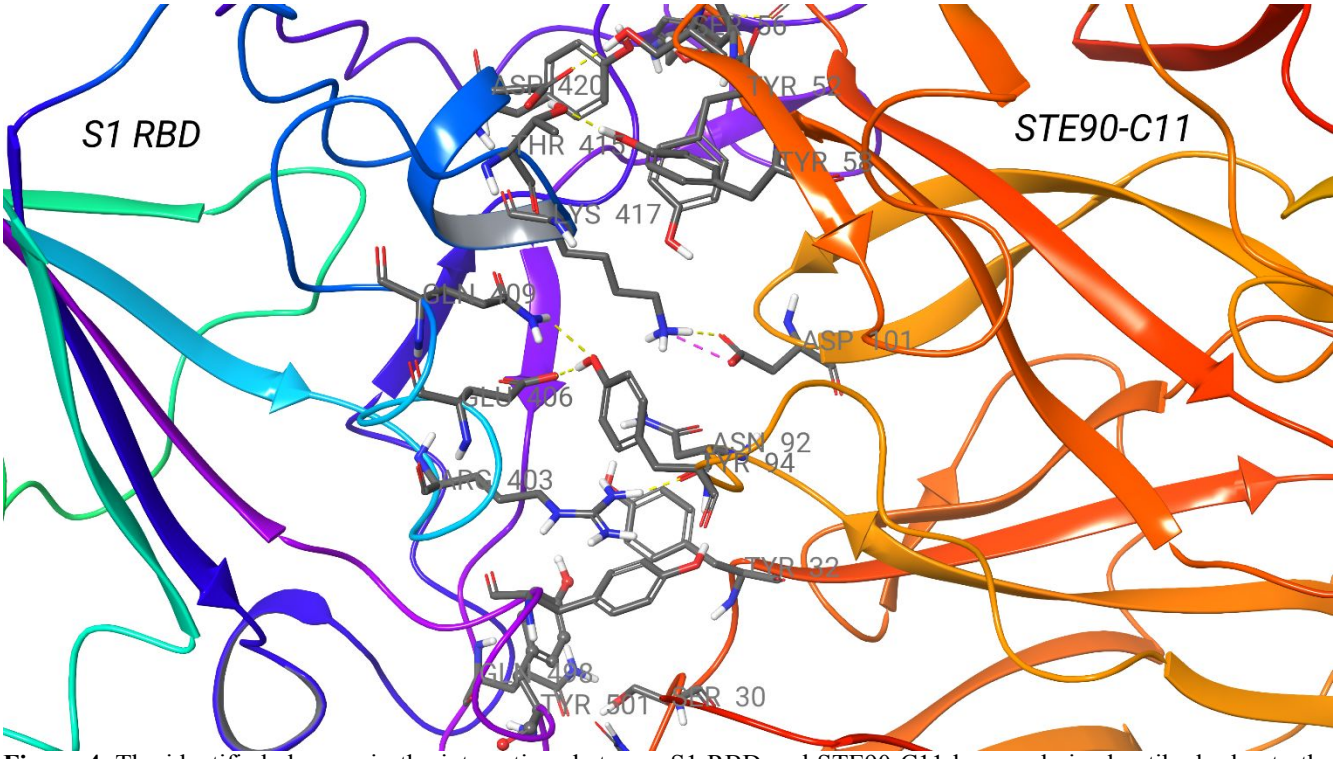

Figure 4. The identified changes in the interactions between S1 RBD and STE90-C11 human derived antibody due to the N501Y mutation. With yellow dot lines are shown the H-bonds.

neutralization assay [12]. This is equivalent to ΔG value of about -12.7 kcal/mol (ΔG=RTln (IC_{50}). Thus, our calculations predict that the N501Y mutant will produce a decrease of the binding into ΔG = -8.92 kcal/mol or 293 nM. This is about 161 times lower than the wild type. The value from extended 15 ns-long FEP simulation was similar: **3.48 kcal/mol**.

2) Initially, we detected an increase of the binding between S1 RBD and human ACE2 by ΔΔG value of only **-0.5 kcal/mol** after 5 ns of FEP calculations. However, considering the decreasing free energy trend of the complex leg (see **Figure 1C**; it decreased by about 1 kcal/mol only for the last 2 ns of the FEP/REST simulations) and our 500 ns-long classical MD simulation we expected this value to be much more significant after extension of the REST sampling to 15 ns. This hypothesis was confirmed and we obtained a ΔΔG value of **-1.75 kcal/mol** from the extended simulation (**Figure 1F**). In support to our data are also the *in vivo* studies of N501Y on mice [2].

3) The addition of K417N mutation led to a dramatic decrease of the STE90-C11 antibody binding to virus's S1 RBD. The default FEP sampling protocol calculated a ΔΔG value of **5.74 kcal/mol**. In the case when both N501Y and K417N mutations are present at the same time this value further increased to 8.61 kcal/mol but this simulation was not well converged and after its extension to 15 ns we obtained a value of **5.83 kcal/mol**. Thus, it seems that the effect of these mutations is not additive and only the K417N mutation can abolish the interaction with STE90-C11 antibody. These results also suggest that even the well tolerated to mutations antibodies eventually would be resisted to this variant of SARS-CoV-2.

4) The K417N mutation also increased the S1 RBD binding to ACE2 after 5 ns of sampling, however, by only -0.39 kcal/mol. The convergence after 5 ns of FEP/REST simulations was better than in the N501Y but after 15 ns of FEP simulations it became clear that in fact K417N decreased the interactions by 0.48 kcal/mol.

These results can be considered as a trustful because our FEP calculations reproduced well the experimental data for selected mutations [**Figure 2** and ref. 12, see Fig 4A]. For instance, for the N501D mutation we calculated a ΔΔG value of **3.54 kcal/mol** meaning that it greatly reduces the S1 RBD binding to ACE2, in accordance to the experimentally observed change of over 100 times. In contrary, the N501T mutation transformed the S1 RBD to a better binder (ΔΔG = **-1.69 kcal/mol**), in an excellent agreement with the experimental data. Additional sets of calculations for other mutations, such as for example the transformation of N501D to N501Y (ΔΔG = **-4.32 kcal/mol**), were also performed in order the CC ΔΔG predictions to be obtained. The latter result provides an additional support that the N501Y mutation increases significantly the binding. In conclusion, it is evident from both the experimental data and FEP study here that the binding of the spike S1 RBD to ACE2 is highly sensitive to the N501 mutations and even the substitutions with small residues, such as N501T, seems to alter the structure of the complex. Based on the all FEP calculations it is also evident that at least 15ns –long FEP/REST simulations for protein selectivity are required for systems with more than 100 000 atoms.

Further, to explain molecular mechanism of observed free energy differences during the FEP calculations we analyzed the N501Y mutated S1 RBD-ACE2 complex. The Tyr501 makes a stable H-bond with the crucial for the ACE2 binding residue Lys353 (**Figure 3**) but our longer 500 ns-long MD simulation showed that this bond is not so pronounced and mainly the hydrophobic interactions and π-π stacking of Tyr501 with Tyr41 of ACE2 increased the binding strength. The Leu455 was in a much closer position to ACE2 interacting with the surface helix residues. A conformational change of other residues were also detected as such for example Tyr449, Tyr453, Gln493, Thr500, Tyr505 and other. These simulations explain also why the G502 and L455 mutations are so sensitive to the ACE2 interactions.

As we shown by FEP calculations the reduction of the S1-RBD binding to STE90-C11 was well pronounced. Thus, we also studied the structural changes due to the N501Y mutation based on most represented structure from the FEP MD ensemble. Two equivalent antibodies can bind to the virus's spike S1-RBD. Thus, the N501Y mutation can affect the binding by both via direct interactions with only one of them and also to produce a change in the interactions between the individual STE90-C11 units.
One of the obvious alters detected was the disruption of the formed by Gln498 H-bond with Ser30. This is also valid for Thr500 – Ser30 hydrogen bond and in general the hydrophobic interactions in this part of the S1 RBD binding surface (see **Figure 3**). Indeed, the Asn501-Ser30 and Gly502-Gly28 H-bonds were also removed. The Tyr501 did not provided any significant interactions with the antibody. The Tyr58 located in the second chain of the antibody dramatically changed its conformation leaving the central point of the binding to the antibody without any stable hydrophobic stabilization and also disrupting the hydrogen bond network formed by Ser56 of the antibody. These changes were introduced because of the Tyr501 stabilization role on the conformation of Arg403 and Arg408. Tyr58-Thr415 and Ser56-Asp420 H-bonds were also altered by the conformation of Tyr58. All of these conformational

changes were not observed during the wild type simulation. These data should be further confirmed by long term MD simulations which are underway in our lab and more details would be revealed.

The mechanism of action of K417N mutation is also clear (see **Figure 4**). After the disruption of the aftermentioned interactions of S1 RBD with STE90-C11, and in particular the conformational change of Tyr58, the Lys417 occupied the same area making a strong hydrogen bond with Asp101. The cancellation of this H-Bond by the asparagine mutation and the other established interactions of Lys417 are an obvious reason for the further decrease in the binding. More MD simulations would be helpful to reveal the additive mechanism of action of N501Y and K417N mutations. The same is valid also for the description of the S1 RBD – ACE2 interactions. Based on the 500 ns-long MD simulation of N501Y mutant we can conclude *the Lys417 seems have a compensatory mechanism of action increasing the free energy by 1.6 kcal/mol*, as shown also per our FEP calculations [6]. It has an important role in the binding and can create a strong H-bonds with Asp30 and His34. However, this is not the real case when both N501Y and K417N mutations are present at the same time and their effect on the S1 RBD conformational changes and S1 RBD-ACE2 binding remains to be revealed.

The main limitation of our study is the investigation of the interactions of only one human derived antibody with the SARS-CoV-2 S1 RBD which falls to class 1 antibodies. However, during our calculations no other experimental structures and information about the binding modes of most frequent plasma antibodies were available; it seems that they have very different S1 RBD binding epitopes. Moreover, the STE90-C11 has been considered as one of most tolerated to the virus mutations antibodies.

The aim of this study was to provide urgently high quality data about the effect of the N501Y and K417N mutations [6]. However, during the process of revision of the paper many experimental studies became available which was an excellent opportunity for a validation of the *in silico* approaches employed here and in particular protein-protein FEP. Also, we can compare our results to other data obtained by theoretical approaches.

Several experimental data about the interactions between hACE2 and RBD became available. They have been obtained by differed methodology and the binding affinities slightly varied between the individual studies. For the N501Y mutation a $\Delta\Delta G_{exp}$ value of **-1.38 kcal/mol** was obtained by fluorescence-activated cell scan [13]. In another study the effect of this mutation on ACE2 binding to RBD has been investigated by biolayer interferometry and a $\Delta\Delta G_{exp}$= **-1.16 kcal/mol** was obtained [14]. The data from the cell surface-binding assay shown $\Delta\Delta G_{exp}$= **-1.67 kcal/mol** [15]. The mean value of these experimental data is **-1.40 kcal/mol** which completely agree with the calculated here value of **-1.42 kcal/mol** by FEP. The further FEP studies performed by other researchers also predicted a correct value of $\Delta\Delta G = -0.81$ kcal/mol, suggesting that the N501Y mutation increases the binding affinity between hACE2 and S1 RBD [13]. Further, the experimental support for the decreased binding affinity of the K417N mutation has been provided: $\Delta\Delta G_{exp}$= **0.56 kcal/mol** which was close to the calculated by us value of $\Delta\Delta G$=**0.64 kcal/mol** [15]. The compensatory mechanism to the binding free energy of K417N to the double N501Y/K417N mutant was also shown to be in an agreement to our calculations [13, 15]. For K417N another FEP study obtained a $\Delta\Delta G$ value of 1.48 kcal/mol [16]. Previously, the FEP calculations provided a helpful insight about the observed enhanced binding of S1 RBD (by factor of 10 to 15) to

ACE2 compared with SARS-CoV identifying the main residues contributing to this change [17]. Between them the Asn501 has been found to decrease the free energy of binding by about -0.5 kcal/mol stabilizing better the S1 RBD of SARS-CoV-2 to the ACE2 by affecting hydrophobic stacking of Tyr41(ACE2)–Lys353(ACE2)–Tyr505 to become more ordered [17]. In a similar way the alanine scanning performed by FEP calculations identified the potential mutations which changed the binding affinity to ACE2 of the new SARS-CoV-2 virus compared to the old one [18]. In these calculations the Asn501 was also detected as a "hot spot". Thus, the mutations in this position in the different virus lineages and types are already known and seems to be common.

The structural basis of the observed changes in the binding activity was not clearly shown by the experimental studies. There is still no structures of the RBD-ACE2 complex with either K417N or N501Y/K417N mutations whereas those of the N501Y mutant with ACE2 (Pdb id: 7BH9) is not so informative due to the artificial introduction of Q498R (this mutation does not exist in current variants) at this microenvironment around Tyr501. The refined by *in silico* approaches structure shown that Y501 of Y501-RBD forms hydrogen bonds with D38 and K353 of ACE2 and the aromatic ring of Y501 also has a strong aromatic stacking interaction (pi stacking) with the aromatic ring of Y41 of ACE2 [13]. It is quite likely that the ring-ring interaction may contribute the much higher binding affinity between Y501-RBD and ACE2 [13]. These results are also quite similar to those obtained by our analysis above.

Many experimental studies about the antibody action became also available. The *in vitro* studies identified that the N501Y and K417N can abolish and/or significantly decrease the binding of several antibodies manly from class 1. Information about the STE90-C11 antibody was not obtained yet but it belongs to class 1. For instance, the activity of CB6 is rendered inactive against B.1.351 because of K417N and the activities of Brii-198 and COV2-2196 are diminished 14.6 fold and 6.3 fold, respectively, against B.1.351 but not against B.1.1.7 lineage [19]. An analysis of 17 class 1 antibody structures revealed their epitopes to be centered on spike residue K417, one of three substitutions in the RBD of the B.1.351 lineage [20]. Three representative antibodies were assessed by ELISA and achieved saturated binding to recombinant RBD from the original lineage but not B.1.351 RBD. Similarly, all three antibodies potently neutralized the original lineage, but not the B.1.351 pseudovirus, confirming dependence on the K417 residue [20]. Five out of the 17 most potent mRNA vaccine-elicited mAbs were at least 10-fold less effective against pseudotyped viruses carrying the K417N mutation [21]. The N501Y mutation causes resistance to mAb COV2-2499 [21], modest effects on binding by majority of other mAb (e.g., COVA1-12 and COVA2-1778 or bamlanivimab/LY-CoV555 [13]), and minor reductions in neutralisation by convalescent sera [20] or sera from individuals vaccinated with BNT162b2. Four out of the 17 most potent mRNA vaccine-elicited mAbs were at least 10-folds less effective against pseudotyped viruses carrying the N501Y mutation [21].
The vaccine effectiveness has been shown to be reduced by the South African variant [13]. The B.1.351 neutralization titer was reduced 8- to 9-fold for Pfizer and AstraZeneca vaccines; they didn't work in a 2 from 25 and 9 of 25 cases, respectively.

All of the aforementioned information clearly showed that our FEP calculations correctly identified the possible escape of class 1 antibodies and the reduction of the vaccine potential. It should be also noted

that another *in silico* study also shown that the K417N mutation fully abolished the CB6 antibody binding; reduces the binding energy by 9.59 kcal/mol [16]. Taken together these data we demonstrated that the FEP calculations can be a precise tool for the prediction of the mutational effect of the protein-protein binding and in particular the SARS-CoV-2 effect of the possible new mutations.

References

[1] K. Kupferschmidt. Mutant coronavirus in the United Kingdom sets off alarms, but its importance remains unclear. *Science*, December 20, **2020**; https://www.sciencemag.org/news/2020/12/mutant-coronavirus-united-kingdom-sets-alarms-its-importance-remains-unclear

[2] Gu H, Chen Q, Yang G, He L, Fan H, Deng YQ, Wang Y, Teng Y, Zhao Z, Cui Y, Li Y, Li XF, Li J, Zhang NN, Yang X, Chen S, Guo Y, Zhao G, Wang X, Luo DY, Wang H, Yang X, Li Y, Han G, He Y, Zhou X, Geng S, Sheng X, Jiang S, Sun S, Qin CF, Zhou Y. Adaptation of SARS-CoV-2 in BALB/c mice for testing vaccine efficacy. *Science* **2020**, 369, 1603–1607.

[3] Abel, R.; Wang, L.; Harder, E.D.; Berne, B.J.; Friesner, R.A., Advancing Drug Discovery through Enhanced Free Energy Calculations. *Acc. Chem. Res*., **2017** 50, 1625-1632.

[4] A. J. Clark, C. Negron, K. Hauser, M. Sun, L. Wang, R. Abel, R. A. Friesner. Relative Binding Affinity Prediction of Charge-Changing Sequence Mutations with FEP in Protein–Protein Interfaces. *J. Mol. Biol*., **2019**, 431, 7, 1481-1493.

[5] Ford MC, Babaoglu K. Examining the Feasibility of Using Free Energy Perturbation (FEP+) in Predicting Protein Stability. *J. Chem. Inf. Model*. **2017** 57, 1276-1285.

[6] Fratev, F. The N501Y and K417N mutations in the spike protein of SARS-CoV-2 alter the interactions with both hACE2 and human derived antibody: A Free energy of perturbation study bioRxiv; 2020. 26 Dec. DOI: 10.1101/2020.12.23.424283

[7] Fratev F, Sirimulla S. An Improved Free Energy Perturbation FEP+ Sampling Protocol for Flexible Ligand-Binding Domains. *Sci. Rep*. **2019**; 9(1):16829.

[8] Zhou R, Das P, Royyuru AK. Single mutation induced H3N2 hemagglutinin antibody neutralization: a free energy perturbation study. *J. Phys. Chem. B*. **2008**, 112,15813-15820.

[9] Harder, E.; Damm, W.; Maple, J.; Wu, C.; Reboul, M.; Xiang, J.Y.; Wang, L.; Lupyan, D.; Dahlgren, M.K.; Knight, J.L.; Kaus, J.W.; Cerutti, D.S.; Krilov, G.; Jorgensen, W.L.; Abel, R.; Friesner, R.A. OPLS3: A Force Field Providing Broad Coverage of Drug-like Small Molecules and Proteins. *J. Chem. Theory Comput*, **2016**, 2, 281–296

[10] F. Bertoglio, V. Fühner, M. Ruschig, P. A. Heine. A SARS-CoV-2 neutralizing antibody selected from COVID-19 patients by phage display is binding to the ACE2-RBD interface and is tolerant to known RBD mutations. *BioRxiv*, **2020**, doi: https://doi.org/10.1101/2020.12.03.409318

[11] Fratev F, Miranda-Arango M, Lopez AB, Padilla E, Sirimulla S. Discovery of GlyT2 Inhibitors Using Structure-Based Pharmacophore Screening and Selectivity Studies by FEP+ Calculations. *ACS Med. Chem. Lett*. **2019**; 10, 904-910.

[12] Starr, T. N., Greaney, A. J., Hilton, S. K., Crawford, K., Navarro, M. J., Bowen, J. E., Tortorici, M. A., Walls, A. C., Veesler, D., & Bloom, J. D. Deep mutational scanning of SARS-CoV-2 receptor binding domain reveals constraints on folding and ACE2 binding. *Cell* **2020**, 182, 5, 3, 1295-1310.e20

[13] Liu H, Zhang Q, Wei P, Chen Z, Aviszus K, Yang J, Downing W, Peterson S, Jiang C, Liang B, Reynoso L, Downey GP, Frankel SK, Kappler J, Marrack P, Zhang G. The basis of a more contagious 501Y.V1 variant of SARS-COV-2. *Cell Res*. **2021** Apr 23:1–3. doi: 10.1038/s41422-021-00496-8

[14] Zhou D, Dejnirattisai W, Supasa P, Liu C, Mentzer AJ, Ginn HM, Zhao Y, Duyvesteyn HME, Tuekprakhon A, Nutalai R, Wang B, Paesen GC, Lopez-Camacho C, Slon-Campos J, Hallis B, Coombes N, Bewley K, Charlton S, Walter TS, Skelly D, Lumley SF, Dold C, Levin R, Dong T, Pollard AJ, Knight JC, Crook D, Lambe T, Clutterbuck E, Bibi S, Flaxman A, Bittaye M, Belij-Rammerstorfer S, Gilbert S, James W, Carroll MW, Klenerman P, Barnes E, Dunachie SJ, Fry EE, Mongkolsapaya J, Ren J, Stuart DI, Screaton GR. Evidence of escape of SARS-CoV-2 variant B.1.351 from natural and vaccine-induced sera. *Cell*. **2021**, 184, 2348-2361.e6

[15] Tian F, Tong B, Sun L. Mutation N501Y in RBD of Spike Protein Strengthens the Interaction between COVID-19 and its Receptor ACE2. *bioRxiv*; **2021**. DOI: 10.1101/2021.02.14.431117.

[16] Luan B, Huynh T. Insights into SARS-CoV-2's Mutations for Evading Human Antibodies: Sacrifice and Survival. *J. Med. Chem*. **2021** Apr 9. doi: 10.1021/acs.jmedchem.1c00311.

[17] Wang Y, Liu M, Gao J. Enhanced receptor binding of SARS-CoV-2 through networks of hydrogen-bonding and hydrophobic interactions. *Proc. Natl. Acad. Sci. U S A*. **2020**, 117, 13967-13974.

[18] Zou J, Yin J, Fang L, Yang M, Wang T, Wu W, Bellucci MA, Zhang P. Computational Prediction of Mutational Effects on SARS-CoV-2 Binding by Relative Free Energy Calculations. *J. Chem. Inf. Model*. **2020**, 60, 5794-5802.

[19] Wang P, Nair MS, Liu L, Iketani S, Luo Y, Guo Y, Wang M, Yu J, Zhang B, Kwong PD, Graham BS, Mascola JR, Chang JY, Yin MT, Sobieszczyk M, Kyratsous CA, Shapiro L, Sheng Z, Huang Y, Ho DD. Antibody resistance of SARS-CoV-2 variants B.1.351 and B.1.1.7. *Nature*. **2021** Mar 8. doi: 10.1038/s41586-021-03398-2

[20] Wibmer, C.K., Ayres, F., Hermanus, T. et al. SARS-CoV-2 501Y.V2 escapes neutralization by South African COVID-19 donor plasma. *Nat. Med.* **2021**, 27, 622–625.

[21] Focosi D, Maggi F. Neutralising antibody escape of SARS-CoV-2 spike protein: Risk assessment for antibody-based Covid-19 therapeutics and vaccines. *Rev. Med. Virol.* **2021** Mar 16.

Graphical abstract